

Computational Fluid Dynamical Model of a Cyclone Separator in Microgravity

Kevin M Crosby and Brad Frye

Department of Physics, Carthage College, Kenosha, WI

Abstract

Collection efficiencies and operational characteristics of a small air cyclone with a low-density lunar dust load are calculated under different gravitational conditions using computational fluid dynamics (CFD) methods. In agreement with our experimental results obtained on a NASA microgravity research aircraft, the collection efficiency is largely independent of the strength of the external gravitational field. We propose a simple analytical model that explains these results.

1 Introduction

An air cyclone is a device that separates particles from a carrier air stream by means of a centrifugal force acting on the particles. The essential geometry of an air cyclone is depicted in Fig. 1. Dust particles, initially entrained in the air flow, enter the tangential inlet near the top of the cyclone, and follow the downward spiral of the air vortex. Centrifugal force and inertial effects act on the particles to move them outward toward the inner wall of the cyclone where they are trapped in the boundary flow. Trapped particles eventually move down the inner wall and are collected in a dust cup at the base of the cyclone while the air flow reverses direction near the base of the cyclone, and exits through the vortex finder at the top of the cyclone.

Air cyclones are a promising technology for first stage air filtration in future lunar habitats where lunar dust mitigation is a mission critical concern. Primary among the advantages of the air cyclone as a potential technology for lunar habitats are design simplicity, the reduced operating costs associated with the lack of consumables (filtration media), and the general robustness against failure of air cyclones due to the lack of moving parts. While much research has been directed at microgravity studies of liquid phase separation in multiphase fluids in liquid cyclones, comparatively little is known about the operation of air cyclones in microgravity [Ahn *et al.*, 2000]. Our experimental work with cyclones in microgravity as part of NASA's Systems Engineering Educational Discovery (SEED) program demonstrated that the operational characteristics of an air cyclone are not significantly different in lunar gravity [Pennington *et al.*, 2008]. This result suggests that further engineering studies are warranted in order to establish the viability of cyclone filtration in lunar habitats. In this paper, we report the results of a computational fluid dynamics (CFD) study of the cyclone used in our experimental work in reduced gravity.

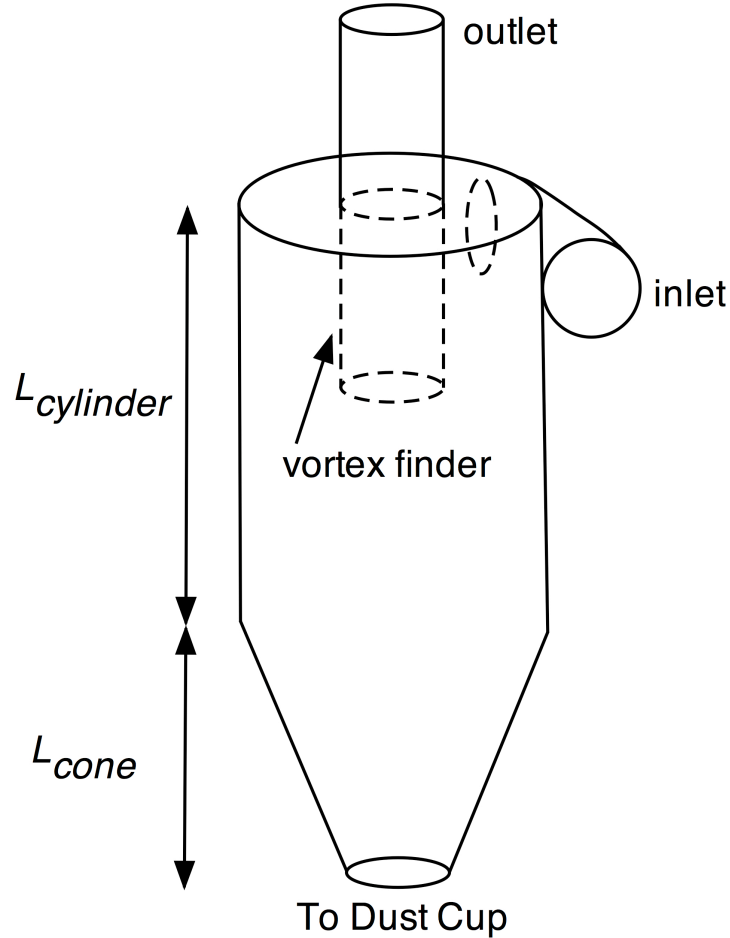


Figure 1: The geometry of the air cyclone used in this study. The cyclone consists of a straight cylinder with diameter 5.08 cm and length $L_{cylinder} = 10.5$ cm, a cone of length $L_{cone} = 14.0$ cm, and a cylindrical vortex finder of diameter 2.54 cm. Dust-laden air is introduced through the inlet of diameter 2.54 cm. A dust cup is attached to the bottom of the cyclone.

2 CFD Workflow and Boundary Conditions

The intent of this study is to model the specific operating characteristics of the cyclone used in our experimental work aboard the NASA C-9 microgravity aircraft. For this reason, we created a geometrically accurate, 3-dimensional CAD model of our cyclone using *SolidWorks* Design software [SolidWorks, Inc.]. Our cyclone is illustrated in Fig. 1. The overall length of the cyclone body is $L = L_{cone} + L_{cylinder} = 24.5$ cm.

The CAD model was imported into *CFDesign* which was used to create the volume mesh for our calculations, and to perform the CFD calculations [Blue Ridge Numerics, Inc.]. The volume mesh consists of 44,500 nodes. *CFDesign* implements the standard $k - \epsilon$ model for evolving solutions of the Navier Stokes equations for turbulent fluid flow [Lauder *et al.*, 1974]. Fluid dynamics in the

context of the $k - \epsilon$ model involves the solution of transport equations for turbulent kinetic energy within the isotropic turbulent viscosity approximation. This model is well-validated for small-scale turbulence, but is known to fail to reproduce accurate inner vortex dynamics in larger cyclones ($L > 1$ m). The failure of the isotropic turbulent viscosity approximation to accurately model flow with high vorticity and turbulent flow that occurs in large systems is not a concern in the present study; our intent is not to accurately reproduce experimental results, but rather to investigate the qualitative features of particle motion in the presence of different gravitational fields.

Boundary conditions for the CFD calculations were derived from the experiments performed on the C-9 aircraft. In particular, an outflow of $v_{\text{out}} = 10.0$ m/s is imposed on the top of the vortex finder, and a zero gauge pressure condition is imposed on the inlet to correspond to the open atmosphere condition in the experiment. The inlet velocity is sufficiently low that the flow can be considered incompressible, greatly simplifying the CFD calculation. The bottom of the cyclone is sealed against losses, while the entire inner surface of the cyclone is presumed to have a coefficient of restitution, $e = 0.5$. A coefficient of restitution, $e < 1$ ensures that particles lose energy on contact with the walls, and so are eventually captured by the walls, as happens in the operation of a real cyclone.

3 Collection Efficiency

The collection efficiency for a cyclone separator is a measure of the relative number of particles trapped in the cyclone at a given particle diameter. Given a discrete spectrum of particle diameters d_i , the collection efficiency for the $i - th$ particle type is:

$$\epsilon_i = \frac{N_i - N'_i}{N_i} \quad (1)$$

where N_i is the number of particles of diameter d_i present at the inlet, and N'_i is the number of particles of diameter d_i that escape collection and exit the cyclone through the vortex finder. In our CFD calculations, we introduce a monodisperse spectrum of particles with diameters between 0.1 and $15 \mu\text{m}$ to the inlet of the cyclone. The particles have mass densities $\rho_p = 2900 \text{ kg/m}^3$, a value chosen to match the mass density of the lunar dust simulant, JSC-1AF used in our experiment [Orbitec, Inc.]. In each calculation run, 100 particles at each diameter are injected into the cyclone with a common initial speed that match the inlet gas flow rate of $V_i = 10.0$ m/s.

Two sets of calculations are performed for each set of particles. In the first calculation, the particles are subject only to the centrifugal and inertial effects that result from their mass. Gravity does not act on the particles in this case. In the second set of calculations, the same spectrum of particles is introduced to the cyclone with the same initial conditions, but with a 1-g gravitational acceleration acting in the axial direction. Representative particle traces for particles of diameter $d_p = 0.1 \mu\text{m}$ and $d_p = 10 \mu\text{m}$ are shown in Fig. 2. The qualitative features of particle motion in a cyclone are reproduced in our CFD calculations. In particular, the smaller mass associated with the $d_p = 0.1 \mu\text{m}$

particles results in reduced centrifugal and inertial forces on the particles, and the particles stay largely entrained in the air flow as it travels through the cyclone. Most of these smaller particles escape with the air through the axial vortex finder. The heavier ($d_p = 10\mu\text{m}$) particles experience larger inertial and centrifugal forces, and travel to the walls of the cyclone where they are eventually trapped.

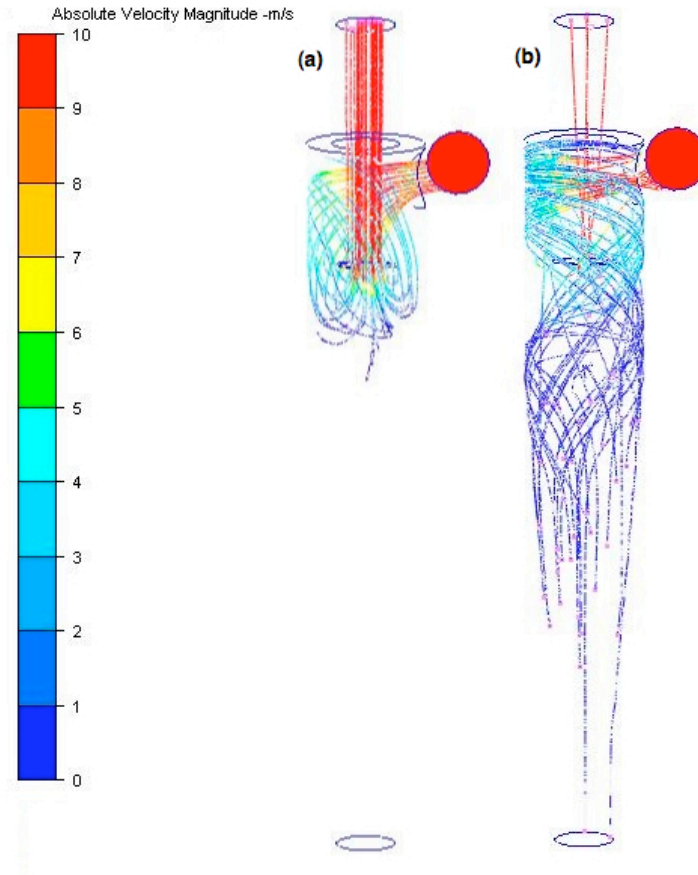


Figure 2: Representative particle traces for particles of diameter (a) $0.1\ \mu\text{m}$, and (b) $10.0\ \mu\text{m}$. The larger particles are more efficiently captured in the cyclone, while most of the smaller particles escape.

Collection efficiencies for each set of particles are calculated according to Eqn. 1. The efficiency results for both zero and 1-g calculations are displayed in Fig. 3. There is no statistically significant difference between the collection efficiencies obtained under the different gravitational fields. This result agrees well with our experimental data which are also displayed in Fig. 3. For particles with $1.0\ \mu\text{m} < d_p < 5\ \mu\text{m}$, the CFD calculations underestimate the efficiency of particle capture relative to experimental data. This is due to the inability of the standard $k - \epsilon$ model to reproduce the strong inner vortex present in real cyclones. In a real cyclone, the inner vortex core extends nearly the entire length of the cyclone and serves to provide particle trajectories that can also span the length of the cyclone. In contrast, the CFD calculations produce an axially compressed inner vortex that results in a “short-circuit” of the flow for particles entrained in the inner vortex. The

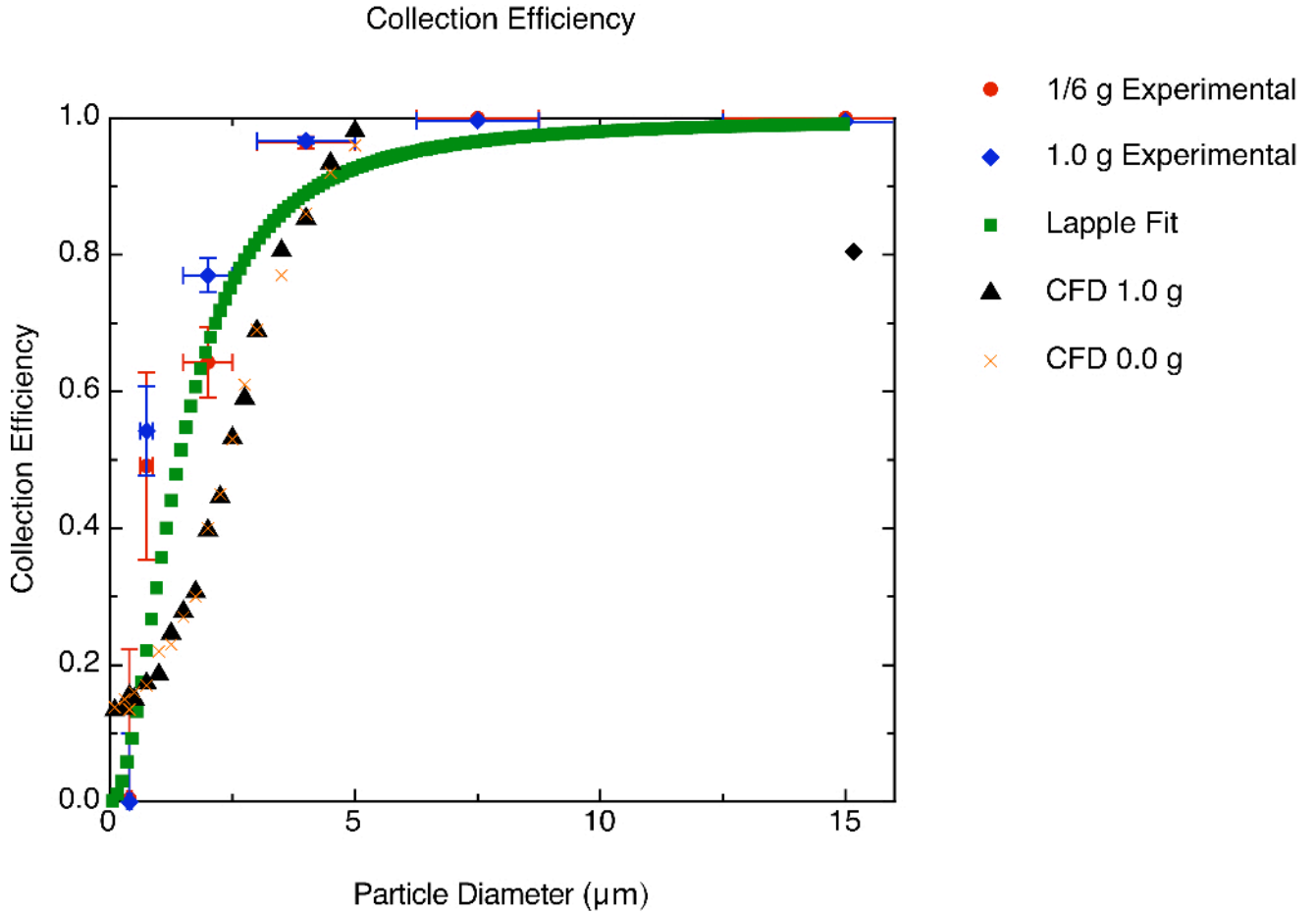


Figure 3: Experimental results (● and ◆), CFD results(▲ and ×), and Lapple Model predictions (■) for the performance of the model cyclone used in this study. The width of the error bars on the experimental data represents the uncertainty in particle size measurements in the particle detector used. The heights of the error bars on the experimental data are the standard deviations of the collection efficiency measurements. The numerical data has sampling errors smaller than the symbol size. The Lapple model data is a fit of the cyclone performance predictions derived from the work in Ref. [Shepherd *et al.*, 1940].

smaller particles do not travel far down the cyclone before the truncated vortex flow carries them out the vortex finder.

4 Analytic Model of Particle Collection

We can understand the somewhat unexpected result that gravity does not play a significant role in particle capture in our cyclone through a heuristic model that incorporates the important physics of particle motion in a vortex flow. We make the reasonable assumptions that (a) the particles do not

interact with each other (low density dust load), and (b) the particles are sufficiently small that they do not affect the flow characteristics. The latter condition leads to a requirement that the air flow is laminar in the presence of the particles, and the drag force acting on the particle is governed by Stokes' Law, $\mathbf{F}_D = -3\pi\eta d_p \mathbf{v}$. Here, $\eta = 1.75 \times 10^{-5}$ Pa-sec. is the kinematic viscosity of dry air, d_p is the particle's aerodynamic diameter, and \mathbf{v} is the particle's velocity.

The motion of a particle initially entrained in the air flow is subject to the forces identified in Fig. 4. Let the density of the carrier air stream be ρ_g , and the particle density be ρ_p . The axial forces are gravity $F_{\text{weight}} = -(\pi d_p^3 \rho_p g / 6) \hat{\mathbf{z}}$, the gravitational buoyancy force, $F_B = (\pi \rho_g d_p^3 g / 6) \hat{\mathbf{z}}$, and a Stokes drag force $F_D = 3\pi\eta d_p \dot{z} \hat{\mathbf{z}}$. In the rotating frame of the particle, the radial forces include the centrifugal force exerted by the air stream, $F_C = (\pi \rho_p d_p^3 r \dot{\theta}^2 / 6) \hat{\mathbf{r}}$, the opposing radial buoyancy force $F'_B = (\pi d_p^3 \rho_g r \dot{\theta}^2 / 6) \hat{\mathbf{r}}$, and the Stokes drag $F'_D = -3\pi\eta d_p \dot{r} \hat{\mathbf{r}}$. For the small particles of interest here, the tangential velocity of the particle is the same as that of the carrier air stream. Finally, we make the simplifying assumption that the tangential motion of the particle is rigid body-like, so that we can define the constant angular speed of the particle as $\omega \equiv \dot{\theta}$.

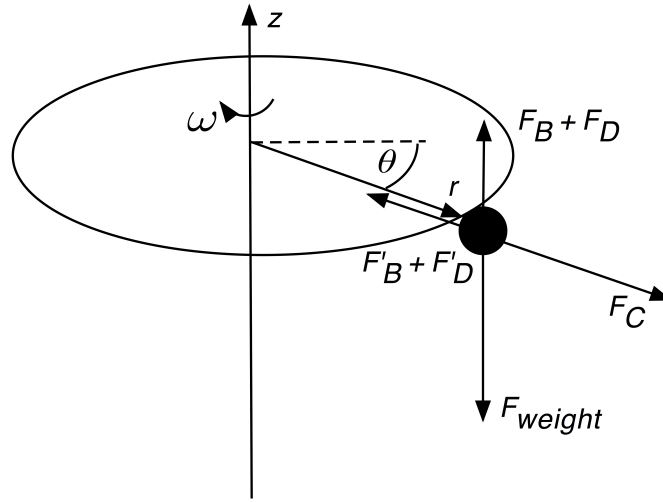


Figure 4: Free body diagram of a particle subject to buoyancy and drag forces in the radial and axial directions. Weight F_{weight} , Stokes drag F_D , and buoyancy force F_B govern axial motion. In the (non-inertial) frame of the particle, an outward centrifugal force F_C acts in opposition to a radial buoyancy force F'_B , and a radial drag force F'_D .

4.1 Axial Motion

For the small particles considered here, axial accelerations act only briefly, and the axial motion of a particle is largely governed by the terminal velocity condition $\ddot{z} = 0$. Force balance in the axial

direction results in the terminal speed

$$v_{zT} \equiv \dot{z}|_{\text{terminal}} = -\frac{(\rho_p - \rho_g)d_p^2}{18\eta}g \quad (2)$$

which is on the order of 10^{-4} m/s for $1 \mu\text{m}$ particles.

4.2 Radial Motion

The radial and tangential motions in the cyclone are coupled, but the analysis simplifies considerably under the rigid body assumption of constant angular speed. In this case, we find the radial motion to satisfy the equation of motion,

$$\ddot{r} = -\left(1 - \frac{\rho_g}{\rho_p}\right)r\omega^2 - \frac{18\eta}{\rho_p d_p^2}\dot{r}. \quad (3)$$

Again, for the small particles considered here, radial accelerations are transient, and we can safely consider the case $\ddot{r} \approx 0$. In this case, Eqn. 3 simplifies to

$$\dot{r} = \frac{(\rho_p - \rho_g)}{18\eta}\omega^2 d_p^2 r. \quad (4)$$

4.3 Residence Time

The residence time of a particle in a cyclone is defined to be the time spent by the particle from entry at the inlet to entrainment at the boundary flow near the wall or dust cup. A particle is considered to have been captured if the particle residence time is less than the residence time of the air as it flows through the cyclone. This condition is a rough guide to expected collection efficiency and results in an empirical estimate of the collection efficiencies for a given particle diameter and a given cyclone geometry. The cyclone consists of two segments, a cylinder with fixed outer radius R , and a cone with radius $R(z)$. We can estimate the residence time of particles in our cyclone by integrating Eqn. 4 from an initial radial coordinate R_0 to the outer radius of the cyclone R . For simplicity, we initially consider motion constrained to the fixed-radius cylinder. Typically, R_0 is considered to be the radius of the vortex finder. We find the particle residence time

$$\tau_{\text{residence}} = \frac{18\eta}{(\rho_p - \rho_g)\omega^2 d_p^2} \log\left(\frac{R}{R_0}\right). \quad (5)$$

Axial and radial motions are decoupled, so that $\tau_{\text{residence}}$ is independent of gravitational acceleration g . It is important to note that, although we've made a gross simplification of the tangential motion by assuming rigid body motion ($\omega \equiv \dot{\theta} = \text{constant}$), the essential result that particle residence times are independent of gravity does not rely on the specific model of tangential motion. In general, the residence time of a particle in a cyclone scales as $(\omega d_p)^{-2}$.

We've assumed that particle motions are confined to the cylinder segment of the cyclone. Relaxing this constraint implies that we consider the wall of the cyclone to be described by the function

$$R(z) = \begin{cases} R & L_{\text{cone}} \leq z \leq L_{\text{cone}} + L_{\text{cylinder}} \\ R_0 + ((R - R_0)/L_{\text{cone}})z & z \leq L_{\text{cone}} \end{cases} . \quad (6)$$

In this case, residence times will be a weak function of z through the $\log(R(z)/R_0)$ dependence, and are therefore weakly coupled to the gravity-driven axial motion (Eqn. 2). We expect in this case that reduced gravity may have a "second order" effect on residence times, slightly reducing capture efficiencies. Our experiments with lunar dust simulant did not have the resolution to discern a difference in collection efficiencies between lunar and earth gravity. We are currently designing more sensitive cyclone experiments that will have the resolution to identify gravitationally induced differences in cyclone performance if they are actually present.

5 Summary and Future Directions

We have performed CFD calculations on a model of the small cyclone separator used in our microgravity experiments on cyclone performance in lunar gravity. Our CFD calculations agree well with the central finding of the experiment: Gravity does not play a significant role in determining collection efficiencies over the range of particles diameters typically present in lunar dust. By means of a simple, heuristic model of particle motion in a cyclone, we can understand these results in terms of the magnitudes of drag and buoyancy forces acting on small particles in the Stokes regime appropriate to our test particles.

The results obtained in this paper suggest that experiments with higher resolution in particle size and collection efficiency may establish useful bounds on the effect of gravity on collection efficiency in full-scale cyclone separators currently being considered for deployment in future lunar habitats.

6 Acknowledgments

The authors are grateful to the Wisconsin Space Grant Foundation and to Carthage College for the financial support of this work. The authors would also like to acknowledge the contributions of Juan Agui at NASA Glenn Research Center for conceiving of and initiating the experimental program of cyclone performance in reduced gravity.

References

- [Ahn *et al.*, 2000] Ahn, H., Tanaka, K, Tsuge, H., Terasaka, K., and Tsukada, K., Centrifugal gas - liquid separation under low gravity conditions, *Separation and Purification Technology* **19**,

121 (2000).

[Blue Ridge Numerics, Inc.] Blue Ridge Numerics, Inc., 650 Peter Jefferson Place, Suite 250, Charlottesville, VA 22911.

[Launder *et al.*, 1974] Launder, B. E. and Sharma, B. I., Application of the energy-dissipation model of turbulence to the calculation of flow near a spinning disc, *Letters in Heat and Mass Transfer* **1**, 131 (1974).

[Orbitec, Inc.] JSC-1AF lunar regolith dust simulant manufactured by Orbitec, Inc. and provided by Juan Agui, NASA Glenn Research Center.

[Pennington *et al.*, 2008] Pennington, C., Martin, E., Sorensen, E., Fritz, I, Frye, B., and Crosby, K. M., Inertial Filtration in Lunar Gravity: SEED Project Report: http://www.carthage.edu/dept/physics/flight/Final_Report.pdf (2008).

[Shepherd *et al.*, 1940] Shepherd, C. B., and Lapple, C. E., Flow Pattern and Pressure Drop in Cyclone Dust Collectors, *Industrial and Engineering Chemistry* **32**, 1246 (1940).

[SolidWorks, Inc.] SolidWorks Corporation, 300 Baker Avenue, Concord, MA 01742.